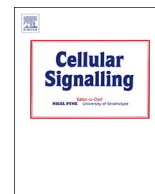




ELSEVIER

Contents lists available at ScienceDirect

## Cellular Signalling

journal homepage: [www.elsevier.com/locate/cellsig](http://www.elsevier.com/locate/cellsig)

# Cannabinoid receptor 2 activation alleviates septic lung injury by promoting autophagy via inhibition of inflammatory mediator release

A.P. Liu<sup>a,1</sup>, Q.H. Yuan<sup>b,1</sup>, B. Zhang<sup>a</sup>, L. Yang<sup>a</sup>, Q.W. He<sup>a</sup>, K. Chen<sup>a</sup>, Q.S. Liu<sup>a</sup>, Z. Li<sup>a,\*</sup>, J. Zhan<sup>a,\*</sup>

<sup>a</sup> Department of Anesthesiology, Zhongnan Hospital of Wuhan University, 430071 Wuhan, Hubei, People's Republic of China

<sup>b</sup> Department of Anesthesiology, Renmin Hospital of Wuhan University, 430060 Wuhan, Hubei, People's Republic of China

## ARTICLE INFO

## Keywords:

Cannabinoid receptor 2  
Autophagy  
Acute lung injury  
Inflammation  
Sepsis

## ABSTRACT

Septic lung injury is one of main causes of high mortality in severe patients. Inhibition of excessive inflammatory response is considered as an effective strategy for septic lung injury. Previous studies have shown that cannabinoid receptor 2 (CB2), a G protein-coupled receptor, play an important role in immunosuppression. Whether CB2 can be used as a therapeutic target for septic lung injury is unclear. The aim of this study is to explore the role of CB2 in sepsis and its potential mechanism. In this study, treatment with HU308, a specific agonist of CB2, could reduce lung pathological injury, decrease the level of inflammatory cytokines and strengthen the expression of autophagy-related gene after cecal ligation puncture (CLP)-induced sepsis in mice. Similar results were obtained in RAW264.7 macrophages after LPS treatment. Furthermore, the effect of HU308 could be blocked by autophagy blocker 3-MA in vivo and in vitro. These results suggest that CB2 serves as a protective target for septic lung injury by decreasing inflammatory factors, which is associated with the enhancement of autophagy.

## 1. Introduction

The endocannabinoid system, which has immunoregulatory properties, has emerged as a promising target for the treatment of numerous diseases, including inflammatory diseases, neurodegenerative disorders, and metabolic syndromes [1]. The endocannabinoid system is composed of cannabinoid receptors, the endogenous ligands, and the enzymatic systems [2,3]. Two major cannabinoid receptors are identified as cannabinoid receptor 1 (CB1) and cannabinoid receptor 2 (CB2). The CB1 is one of the most abundant G protein-coupled receptors in the brain whereas the CB2 is mostly expressed in peripheral organs with immune function [4]. CB2 agonists have been used as an attractive drug for the treatment of many diseases. For example, CB2 activation could reduce release of pro-inflammatory mediators in rheumatoid arthritis [5], and activation of CB2 had a decrease in myocardial inflammation and oxidative stress [6]. However, there are still some conflicting results regarding the effects of CB2R activation particularly with specific regard to the complex disease progression of sepsis [7,8]. Therefore, the specific contribution of CB2R to sepsis and the underlying mechanism needs to be further explored.

Sepsis is a common syndrome of multiorgan dysfunction characterized by an imbalance between pro-inflammatory and anti-

inflammatory factors in response to a systemic infection [9]. Among the injured organs, the lung is one of the most vulnerable target organs in sepsis. The sepsis-associated acute lung injury (ALI) is manifested as inflammatory cell infiltration, endothelial cell damage, and pulmonary edema. Unfortunately, there are no approved effective preventive strategies or treatment options available for the treatment or prevention of ALI [10–12]. Autophagy is an evolutionarily conserved catabolic mechanism, which is recognized as one of the major pathways for degradation and recycling of cellular constituents [13]. Accumulating evidence shows that autophagy is involved in the regulation of cell survival process in response to multiple stresses and is also important for maintaining cellular homeostasis [14,15]. Autophagy as an immunological process is activated initially in sepsis, followed by a subsequent dysfunctional response to infection. Recent studies showed that autophagy plays a protective role in multiple organ injuries partly by regulating inflammation, inhibiting apoptosis and suppressing immune reactions [16–18]. These findings suggested that the autophagic machinery participated in the pathogenesis of sepsis and may serve as a potential therapeutic target for sepsis.

It has been reported that CB2 activation protects from alcoholic liver diseases by inhibiting hepatic inflammation through an autophagy-dependent pathway [19]. However, in ALI induced by sepsis,

\* Corresponding authors at: Department of Anesthesiology, Zhongnan Hospital of Wuhan University, East-Lake Road 169, Wuhan 430071, Hubei, China.

E-mail addresses: [1548205583@qq.com](mailto:1548205583@qq.com) (A.P. Liu), [lz\\_gdwh@126.com](mailto:lz_gdwh@126.com) (Z. Li), [anpeng19950808@163.com](mailto:anpeng19950808@163.com) (J. Zhan).

<sup>1</sup> Co-first authors: Liu AP and Yuan QH, contributed equally to the writing of the article.

whether autophagy is involved in the beneficial effect of CB2 for limiting inflammation remains controversial. In the current study, we explored the mechanism underlying the protective effects of CB2 against ALI. Using autophagy inhibitor, we further demonstrate that autophagy is a key mediator of the anti-inflammatory properties of CB2 in sepsis-induced ALI.

## 2. Materials and methods

### 2.1. Animals and experimental model

SPF male C57BL/6 mice, aged 8–10 weeks, weighing 20–25 g, were purchased from Beijing Vital River Laboratory Animal Technology Co., Ltd. (Beijing, China). The mice were housed in cages on a 12 h light/dark cycle, with the room temperature kept at 20–25 °C and relative humidity at 40–60%. They were allowed free access to a standard diet of rodent chow and drinking water. All experiments were approved in accordance with the guidelines of the Animal Care Committee of Zhongnan Hospital, Wuhan University.

Cecal ligation and puncture (CLP) model was created to induce septic ALI as previously reported [20]. Briefly, male mice were anesthetized with pentobarbital sodium (60 mg/kg, administered intraperitoneally). Then the cecum was ligated with a 4–0 silk suture, punctured with a 20-gauge needle, and a small amount of cecal contents were extruded from the perforation sites. At last, incisions were closed in layers. In the Sham and drug alone group, mice were underwent laparotomy but without CLP.

### 2.2. Culture and treatment of macrophages

Murine macrophage RAW264.7, purchased from the Cell Bank of the Chinese Academy of Sciences, was cultured in a humidified incubator with Dulbecco's Modification of Eagle's Medium (DMEM) (Gibco, USA) supplemented with 10% fetal bovine serum (Gibco, USA) at 37 °C with 5% CO<sub>2</sub>. Cells were seeded with the density of 1 × 10<sup>5</sup> cells/ml.

### 2.3. Reagents

HU308 (a specific agonist of CB2) and AM630 (a specific antagonist of CB2) were purchased from APExBIO Technology (APExBIO, Houston, USA). 3-Methyladenine (3-MA, an autophagy inhibitor) was from MedChemexpress CO.,Ltd. (Medchemexpress CO.,Ltd., USA). Methyl thiazolyl tetrazolium (MTT) was provided by Amresco Inc. (Amresco Inc., Ohio, USA). LDH kit was from Nanjing Jiancheng Bioengineering Institute (Nanjing Jiancheng Bio, Nan Jing, China). Trizol reagent was purchased from Invitrogen Life Technologies (Invitrogen Life Technologies, Grand Island, NY, USA). ReverTra Ace qPCR RT Kit and SYBR Green Real-time PCR Master Mix were from Toyobo Co., Ltd. (TOYOBO CO., LTD, OSAKA, JAPAN). Enzyme-linked immunosorbent assay (ELISA) Kits were provided by Bio-Swamp Life Science Lab (Bio-Swamp, Wuhan, China). Antibody against LC3B (Microtubule Associated Protein 1 Light Chain 3 Beta), Beclin1 and p62 were purchased from Abcam Inc. (Abcam Inc., Cambridge, United Kingdom).

### 2.4. Lung histology analysis

After the mice were sacrificed, the lungs were quickly removed and immersion-fixed in 4% phosphate-buffered saline-buffered formalin. The lung tissues were embedded in paraffin, sectioned, and stained with hematoxylin-eosin using standard histological techniques. Pathological changes and lung injury score was observed and performed under light microscope. Briefly, 10 pulmonary regions were randomly chosen per sample and graded on a scale of 0–4 (0, absent and appears normal; 1, light; 2, moderate; 3, strong; 4, intense) for inflammation, edema, necrosis, hemorrhage and hyaline membrane formation. The assessments

were performed by two pathologists blinded to experimental groups. The lung injury was then calculated based on the mean score [21].

### 2.5. Respiratory index PaO<sub>2</sub>/FiO<sub>2</sub> (arterial oxygen pressure/fraction of inspired oxygen)

At 12 h after surgery, a cervical incision was made. Blood samples were collected by inserting into the right common carotid artery through a stretched PE10 polyethylene catheter filled with heparinized saline. Blood gas analysis was performed for examining respiratory index.

### 2.6. Cell viability

Cell viability was assessed by the methyl thiazolyl tetrazolium (MTT) conversion test. Briefly, RAW264.7 macrophages were seeded on 96-well microtiter plates and allowed to adhere for 24 h. After incubation, 20 µl/well of MTT solution (5 mg/ml) was added and incubated for 4 h. The medium was aspirated and replaced with 150 µl/well of dimethyl sulfoxide solution (DMSO). The plates were shaken for 10 min, and absorbance was determined at 490 nm using an automated microplate reader (RT-6000, Shenzhen Rayto Life Science Limited Company, China). Each assay was performed in ten pores.

### 2.7. LDH determination

Culture supernatants of RAW264.7 macrophages were collected for determination of LDH as an indicator of cell survival. The levels of LDH were measured by 2, 4-dinitrophenylhydrazine chromogenic assay according to the manufacturer's instructions.

### 2.8. Reverse transcription and real-time PCR analysis

Total RNA was extracted from lung tissues and RAW264.7 macrophages using Trizol reagent according to the manufacturer's instructions. The RNA was subjected to reverse transcription with ReverTra Ace qPCR RT Kit. Real-time PCR was conducted in the CFX Connect™ quantitative PCR apparatus (Bio-Rad, CA, USA) using the SYBR Green Real-time PCR Master Mix. GAPDH was used as an internal control for normalization of RNA quantity and quality differences in all samples. The sequences of the primer pairs were as follows:

GAPDH: 5'-TGGAAGGACTCATGACCACA, TTCAGCTCAGGGATGACCTT-3';

CB2: 5'-CGGCTAGACGTGAGGTTGGC, GGCTCTAGGTGTTTTT CAC-3';

TNF-α: 5'-CCCTCACACTCAGATCATCTTCT, GCTACGACGTGGGCT ACA-3';

IL-1β: 5'-GCAACTGTTCCCTGAACTCAACT, ATCTTTGGGGTCCGTC AACT-3';

IL-18: 5'-GACTCTTGCCTCAACTTCAAGG, GCAACTGTTCCCTGAACT CAAC-3';

Atg5: 5'-AGCCAGGTGATGATTCACGG, GGCTGGGGGACAATGC TAA-3';

Atg7: 5'-GTTCCGCCCTTTAATAGTGC, TGAACCCAACGTCAAG CGG-3';

Beclin1: 5'-ATGGAGGGGTCTAAGGCGTC, TCCTCTCTGAGTTAGC CTCT-3';

LC3B: 5'-TTATAGAGCGATAACAAGGGGGAG, CGCCGTCTGATTATC TTGATGAG-3';

p62: 5'-AGGATGGGGACTTGGTTGC, TCACAGATCACATTGGGG TGC-3';

NLRP3: 5'-ATTACCCGCCGAGAAAGG, TCGCAGCAAAGATCCACA CAG-3'.

### 2.9. Immunohistochemical staining

Lung tissues of mice were deparaffinized and rehydrated in alcohol.

Slides were heated at 110 °C for 8 min in citric acid (pH 6.0) antigen retrieval buffer followed by 7 min at 95 °C and then cooled to 20 °C. The slides were placed in 3% hydrogen peroxide solution and incubated at room temperature without light for 25 min. Then the slides were washed with phosphate buffered saline (PBS) before blocking with 5% bovine serum albumin in phosphate buffered saline-Tween-20 (PBST), and incubated with primary antibodies (anti-Atg5, 1:100, ProteintechGroup, Inc., Wuhan, China) overnight at 4 °C. After being washed, the slides were incubated with horseradish peroxidase (HRP)-labeled secondary antibody (1:100, Aspen) at room temperature for 50 min. Each section was stained with diaminobenzidine (DAB) and counterstained with hematoxylin after being washed. The positive-staining sections were analyzed with the Image pro-plus 6.0 automatic image analysis system. Five high-power fields were randomly chosen to obtain the mean values.

### 2.10. Immunofluorescence staining

Lung tissues were deparaffinized and rehydrated in alcohol and RAW 264.7 macrophage were seeded on coverslip-bottom dishes for 24 h, followed by fixation with 4% paraformaldehyde. The slides were then rinsed with PBS before blocking with 5% bovine serum albumin in PBST, and incubated overnight at 4 °C with primary antibodies. The primary antibodies used were as follows: rabbit anti-LC3 (1:100, Abcam), rabbit anti-LAMP-2(1:100, Aspen), rabbit anti-NLRP3 (1:100, Abcam). After being washed three times with PBS, slides were incubated with the fluorescein isothiocyanate (FITC) or Cy3-labeled goat anti-rabbit IgG secondary antibody (1:100, Aspen) at room temperature for 1 h. After being washed, slides were exposed to DAPI (Beyotime Institute of Biotechnology, China) in dark at room temperature for 10 min. The slides were sealed to microscope slides with anti-fluorescence quenching sealed tablets.

### 2.11. ELISA analysis

Supernatant of RAW264.7 macrophages was harvested from each group after the treatment. Using commercially available kits, TNF- $\alpha$ , IL-18 and IL-1 $\beta$  levels were measured by a two-step sandwich ELISA method, according to the manufacturer's instructions. Background absorbency of blank wells was subtracted from the standards and unknowns prior to determination of sample concentrations. The standard curve and regression equation were calculated, and the absorbance value was substituted into the standard curve to calculate the protein concentrations of inflammatory mediator in each group.

### 2.12. Western blot analysis

The lysates with RIPA buffer (Sigma, USA) containing a mixture of protease inhibitor cocktail kit (Roche, Germany) was used to lyse the lung tissues and RAW264.7 macrophages for 30 min. The tissues and cells were then lysed for 30 min with a non-contact, fully automatic ultrasonic crusher. The concentrations of proteins were measured by BCA protein assay kit (Shanghai, China). Equal amounts of proteins were loaded onto SDS-polyacrylamide gel. Separated proteins were transferred to PVDF membranes and incubated with primary antibody overnight at 4 °C.  $\beta$ -actin polyclonal antibody (Proteintech Group, Inc., Wuhan, China) was used to monitor protein loading. Excess antibody was then removed by washing the membranes in TBST, and the membranes were incubated in HRP-labeled secondary antibody (1:10000, Proteintech Group, Inc., Wuhan, China) for 2 h. After being washed in TBST the bands were detected by enhanced chemiluminescence (ECL) and Image-pro Plus 6.0 image analysis software was used to quantify the density of the individual bands.

### 2.13. Statistical analysis

All measurement data were presented as mean  $\pm$  SD. One-way ANOVA was used for statistical analysis to compare values among all groups, followed by the Student-Newman-Keuls Q test and Dunnett's T3 test to measure the differences between any two groups. Data were analyzed using SPSS 21.0 software. Non-parameter rank test was used for the lung injury scores, and Kaplan-Meier method was used for the comparisons of survival rates. *P*-values < .05 were considered to be statistically significant.

## 3. Results

### 3.1. CB2 activation protected against sepsis-induced ALI in mice

Male mice were randomly divided into six groups: sham, HU308 alone (HU308), AM630 alone (AM630), CLP, CLP treated with HU308 (CLP + HU308), and CLP treated with AM630 (CLP + AM630). In CLP + HU308 and CLP + AM630 group, mice were intraperitoneally injected with 2.5 mg/kg HU308 or AM630 at 15 min after the CLP procedure. An equal volume of saline was intraperitoneally injected in sham and CLP group. In HU308 and AM630 group, mice were intraperitoneally injected with 2.5 mg/kg HU308 or AM630 at 15 min after sham procedure. Then mice were killed at 12 h after surgery, and lung injury scores were examined as mentioned above.

Compared with sham group, there were no differences in HU308 and AM630 groups. The alveolar edema, lung hemorrhage, necrosis and the inflammatory cells infiltration were aggravated in CLP group. As shown in Fig. 1A, the lung injury induced by CLP was attenuated significantly in HU308-treated mice, as evidenced by reduced alveolar edema, less inflammatory cell infiltration, and lower levels of lung hemorrhage and necrosis in the lungs, while AM630 has no effect.

Another sixty mice were randomly assigned to six equal groups to observe survival status during 96 h after CLP. The cumulative survival curve was depicted using the Kaplan-Meier method. Administration of HU308 and AM630 alone after sham surgery both revealed 100% survival rates the same as sham group (Fig. 1B). Post-administration of HU308 conferred significant protection from sepsis, while AM630 has no effect on the survival rates of mice compared with CLP-treated mice.

PaO<sub>2</sub>/FiO<sub>2</sub> (oxygenation index), was measured as an index of lung injury when its value was less than or equal to 300 mmHg. As shown in Fig. 1C, compared with sham group, there were no significant differences in HU308 and AM630 alone groups, while oxygenation index was obviously decreased at 12 h post-CLP. Compared with CLP group, post-administration of HU308 could improve oxygenation index, while AM630 has no effect.

### 3.2. The effects of autophagy in attenuating CLP-induced inflammatory response by CB2 activation in model mice

As CB2 inhibition by AM630 showed no impact on ALI in our mice model, we used only the agonist HU308 in the subsequent experiments. Then mice were randomly divided into four groups: sham, CLP alone (CLP), CLP treated with HU308 (CLP + HU308), and CLP treated with HU308 plus 3-MA (CLP + HU308 + 3-MA). In CLP + HU308 + 3-MA group, mice were intraperitoneally injected with 10 mg/kg 3-MA at 15 min after the CLP procedure, and injected with 2.5 mg/kg HU308 at 15 min after the 3-MA injection.

The expression of CB2, TNF- $\alpha$ , IL-18 and IL-1 $\beta$  mRNA in lung tissues increased during sepsis-induced ALI. HU308 were shown to play a protective role in sepsis-induced ALI through specifically activation of CB2 by inhibiting inflammatory release in lung tissues (Fig. 2A-D).

Next, we evaluated whether CB2 activation could modulate autophagy proteins in the context of the CLP model. Western blot, immunofluorescence analysis and immunohistochemical staining showed the expressions of autophagy associated proteins Atg5, LC3B-II/LC3B-I

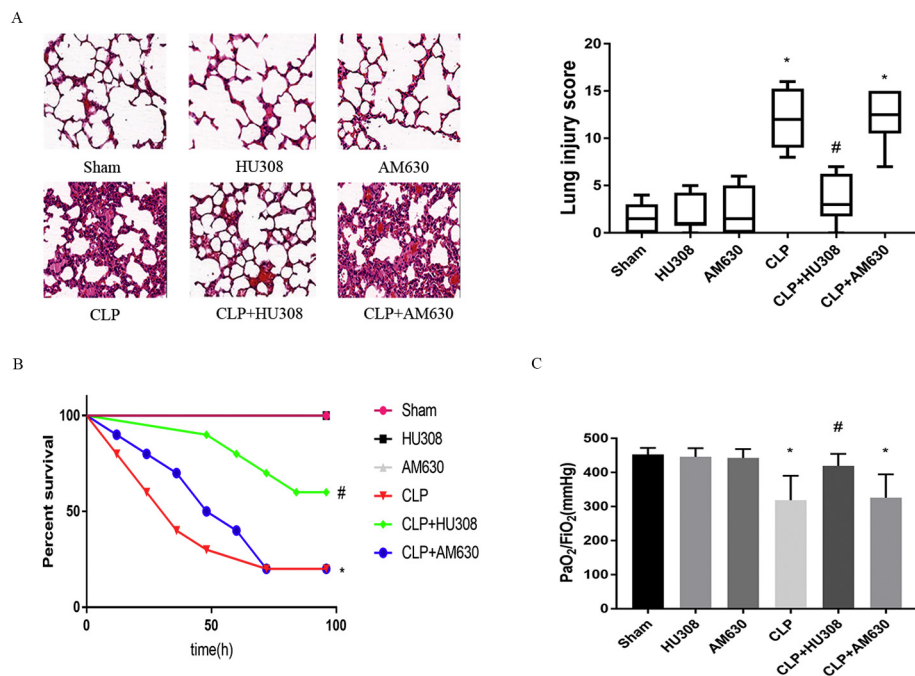


**Fig. 1.** CB2 activation ameliorates CLP-induced ALI in mice.

All of these mice were sacrificed at 12 h after different treatment and lung tissue sections were made and stained with hematoxylin and eosin. (A) Representative photomicrographs ( $\times 200$ ) were shown and the severity of histopathological changes in the lung tissues was scored by observing the morphological structure ( $n = 3-5$ ). Scale bars, 200  $\mu\text{m}$ . (B) The survival rates were monitored for 96 h in each group ( $n = 10$ ). Values are shown as survival percentage. (C) Oxygenation index ( $\text{PaO}_2/\text{FiO}_2$ ) in each group was measured as an index of lung injury ( $n = 8-10$ ). \* $P < 0.05$  versus Sham group; # $P < 0.05$  versus CLP group. CB2: Cannabinoid receptor 2; CLP: cecal ligation puncture.

ratio and Beclin1 in the lungs were further increased, and the expression of p62 was further decreased, as well as the integration of LC3B with LAMP-2 was enhanced after HU308 treatment in comparison with that in CLP group (Fig. 2E-J).

We hypothesized that the enhancement of autophagy was responsible for the protective effects of CB2 activation in attenuating the release of inflammatory cytokines after CLP-induced sepsis. To test this hypothesis, we used autophagy inhibitor 3-MA to block autophagic activities as demonstrated by attenuation of Atg5, LC3B-II/LC3B-I ratio and Beclin1 expressions as well as enhancement of p62 expression and the integration of LC3B with LAMP-2. We found that the protective effects of CB2 activation against CLP-induced inflammatory responses were constrained by 3-MA treatment.

### 3.3. Activate CB2 attenuated cell injury in LPS-stimulated RAW264.7 macrophages

As macrophages were the most typical cells in inflammation, we chose RAW264.7 for the subsequent studies.

RAW264.7 macrophages were divided into six groups: control, HU308 alone, 3-MA alone, LPS, LPS + HU308, and LPS + HU308 + 3-MA. Cells were treated with 1  $\mu\text{g}/\text{ml}$  LPS (Sigma, USA) for 15 min in LPS group, LPS + HU308 group and LPS + HU308 + 3-MA group. In LPS + HU308 + 3-MA group, cells were treated with 3-MA (10 mM) for 15 min, then added with HU308 (10  $\mu\text{M}$ ). In LPS + HU308 group, cells were treated with HU308 (10  $\mu\text{M}$ ). An equal volume of medium was added in control group.

Mitochondrial succinate dehydrogenase in living cells could convert MTT into visible formazan crystals during incubation. The formazan crystals were then solubilized in DMSO. These reactions do not occur in dead cells. Thus absorbance represents the number of surviving cells. As shown in Fig. 3A, HU308 or 3-MA alone exerted no cytotoxic effect on cell survival, and cell survival significantly decreased after LPS challenge. Compared with LPS group, cell survival significantly increased in LPS + HU308 group. However, the increase was diminished in LPS + HU308 + 3-MA group.

The level of LDH is a pathological manifestation associated with cell death. As shown in Fig. 3B, after 24 h, an increase in LDH level was detected after 1  $\mu\text{g}/\text{ml}$  LPS stimulation compared with control group. Compared with LPS group, there was a measurable decrease in

LPS + HU308 group. However, the decrease was disappeared in LPS + HU308 + 3-MA group.

### 3.4. The effects of autophagy in attenuating LPS-induced inflammatory response by CB2 activation in RAW264.7 macrophages

We investigated the contribution of CB2 on LPS-induced inflammation. RAW264.7 macrophages were divided into four groups: control, LPS, LPS + HU308, and LPS + HU308 + 3-MA.

LPS increased the levels of CB2, TNF- $\alpha$ , IL-18, and IL-1 $\beta$ , as well as NLRP3 expressions (Fig. 4A-D). As compared to LPS group, CB2 activation displayed anti-inflammatory response, as reflected by lower expression of pro-inflammatory factors. Meanwhile, we also evaluated the effect of CB2 on autophagic activities shown as Atg5, Atg7, LC3B, Beclin1 and p62 expressions and the ratio of LC3B-II/LC3B-I, indicating that CB2 activation could increase autophagy in vitro (Fig. 4E-G).

Similarly, to confirm whether the protective effects of CB2 activation were involved in attenuating the release of inflammatory cytokines by regulating autophagy, we used autophagy inhibitor 3-MA and observed its effectiveness in LPS-stimulated RAW264.7 macrophages. As shown in Fig. 4, 3-MA treatment dismissed the effort of HU308 in decreasing of inflammatory mediator levels.

## 4. Discussion

In this study, we have demonstrated the protective effect of CB2 activation against sepsis using a mouse model of CLP and LPS-stimulated macrophages. Our findings focused on the potential of CB2 as a new therapeutic target for sepsis. Activation of CB2 attenuates the inflammatory reaction induced by CLP and LPS, in part, through the enhancement of autophagy.

CB2 as a G-protein coupled receptor, have been implicated in progression of clinical diseases such as sepsis and acute kidney injury [22,23]. CB2 activation is immunosuppressive, which might be beneficial during the hyper-inflammatory phase of sepsis [24]. Studies have shown that CB2 can inhibit inflammation, and the major actions may be related to the modulation of the endothelial inflammatory activation [25], inhibition of monocyte migration [26], inhibition of inflammatory proliferation and migration of vascular smooth muscle cells [27], and down-regulation of T cell activation levels [28]. Lehmann C

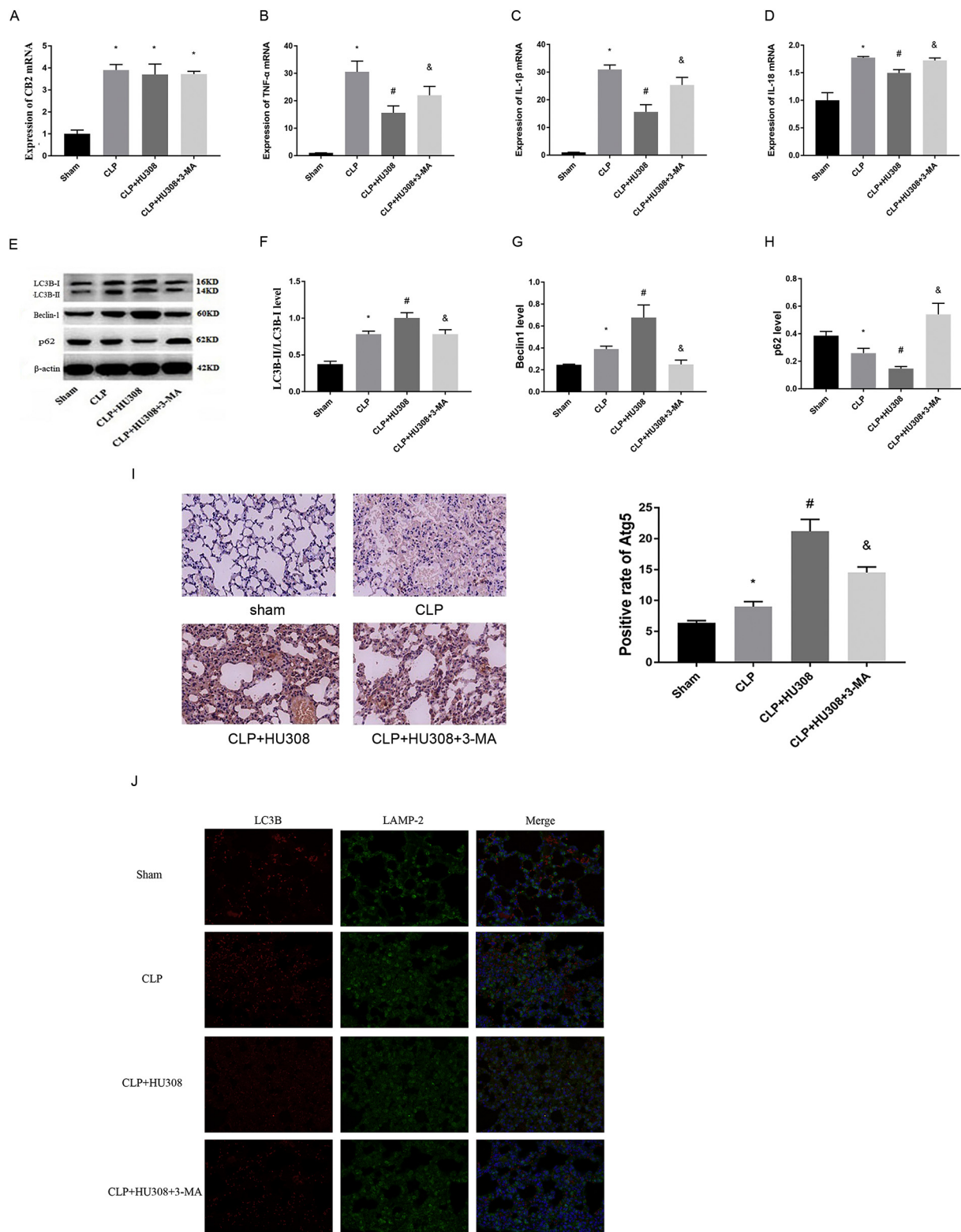


**Fig. 2.** The protective effects of CB2 activation against CLP-induced inflammatory responses were constrained by inhibition of autophagy in mice. All of these mice were sacrificed at 12 h after different treatment and lung tissue was collected for detecting inflammatory factors and autophagy-related indicators. (A) The expression of CB2 mRNA was up-regulated after CLP administration. (B-D) The expression of TNF- $\alpha$ , IL-18 and IL-1 $\beta$  mRNA was measured by qRT-PCR. (E-H) The level of autophagy-associated protein LC3B, Beclin1 and p62 was measured by Western blot analysis. (I) Atg5 was measured by immunohistochemical staining and positive rate of Atg5 was shown. Magnification: 20 $\times$ , Scale bar: 100  $\mu$ m. (J) Integration of LC3B with LAMP-2 was measured by immunofluorescence double staining. Magnification: 40 $\times$ , Scale bar: 20  $\mu$ m. Data are represented as mean  $\pm$  SD ( $n = 3-5$ ), \* $P < 0.05$  versus Sham group; # $P < 0.05$  versus CLP group; &  $P < 0.05$  versus CLP + HU308 group. CB2: Cannabinoid receptor 2; CLP: cecal ligation puncture.

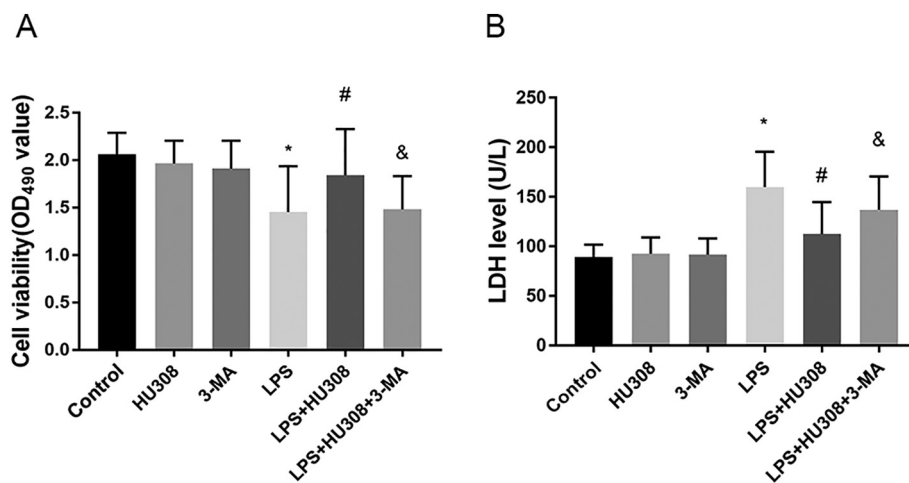


**Fig. 3.** Cell injury in LPS-stimulated RAW264.7 macrophages was attenuated by CB2 activation. Cell viability and LDH level were used to assess LPS-induced cell injury. RAW264.7 macrophages and cell supernatant were collected to measure cell viability and LDH level, respectively. (A) The cell viability was determined using a MTT assay. We also added HU308 (10  $\mu$ M) and 3-MA (10 mM) alone group in order to investigate the cytotoxic effect of these two drugs. (B) LDH levels in different groups. Data are represented as mean  $\pm$  SD (n = 10), \* $P$  < 0.05 versus control group; # $P$  < 0.05 versus LPS group; & $P$  < 0.05 versus CLP + HU308 group. CB2: Cannabinoid receptor 2; LPS: lipopolysaccharide.

et al. found that CB2 expression was upregulated during sepsis and CB2 activation could reduce intestinal leukocyte recruitment and systemic inflammatory mediator release [29]. Similarly, our results also showed that CLP or LPS exposure increased the expression levels of CB2 mRNA. Simultaneously, activating CB2 with HU308 significantly alleviated lung injury and improved survival status in septic mice. Consistently, HU308 treatment resulted in significant decreasing in pro-inflammatory mediator (TNF- $\alpha$ , IL-18 and IL-1 $\beta$ ) levels following CLP exposure, demonstrating that CB2 activation exerted a protective role through inhibiting pro-inflammatory mediator generation.

Autophagy, a major intracellular digestion system, is important in innate immunity, as it is responsible for the clearance of various pathogens [30]. Autophagy is also a complicated biological process involving multiple steps, each of which is coordinated by specific genes, such as Beclin-1, autophagy-related gene 5 (Atg5) and microtubule-associated proteins light chain 3B (LC3B) [31]. There are growing evidences that autophagy is critical for the control of inflammatory responses. Previous study indicated that LPS-induced sepsis could stimulate the increasing of autophagy protein LC3B in kidney tissues [32]; moreover, impaired autophagy may contribute to neuromuscular dysfunction in CLP-induced sepsis [18]. Consistent of these results, our results also showed that there were significant increases in the autophagy-related genes Atg5, LC3B, Beclin1 and decrease in p62 expression after ALI induced by CLP operation. This study indicated that autophagy is potentially involved in inflammation during sepsis-induced ALI.

As CB2 inhibition by AM630 showed no impact on ALI in our model, we used only the agonist HU308 in the subsequent experiments. To clarify the relationship between CB2 activation and autophagy in sepsis, we determined the autophagy status in CLP-treated mice with HU308, and found that HU308 could increase the expressions of autophagy-related genes. To explore the role of autophagy in CB2 protection against sepsis, we further used autophagy inhibitor 3-MA. Blocking autophagy by 3-MA dismissed the effort of HU308 in reducing inflammatory mediator release.

Utilizing CB2 as pharmacological targets to modulate the autophagic activity is a promising strategy for the treatment of different patho-physiological conditions and diseases [33]. Accumulating evidences link activation of CB2 to inflammation via the regulation of autophagy. For example, knocking out CB2 led to a detrimental effect by decreasing the level of autophagy in heart tissues from myocardial infarction mice [34]. Another study showed that activating CB2 by HU308 improved cardiac function through enhancing the level of autophagy in the heart tissues from diabetic cardiomyopathy mice [35]. In keeping with these results, our study also found a significant reduction of the inflammatory mediator production in CLP + HU308 mice. Furthermore, we also observed that the beneficial effects of CB2 agonists could be attenuated by the reduction or inhibition of

autophagy. Several groups have shown that blockade of autophagy attenuated the protective effects of HU308 on different diseases [36,37]. In support of this hypothesis, our data also provided evidence that HU308 suppressed the expression of inflammatory mediators via autophagy induction, suggesting that autophagy induction contributes to the modulation of inflammatory responses by CB2 activation.

The NOD-like receptor family (NLR) protein NLRP3 is an intracellular signaling molecule, whose activation is implicated in the inflammatory process in ALI, by cleavage of downstream secretion of mature IL-1 $\beta$  and IL-18 [38,39]. Mechanistically, we identify NLRP3 as the mediator of autophagy increased by CB2. In order to test this hypothesis, we then used LPS-stimulated macrophages in our *in vitro* study. Activating CB2 with HU308 inhibited NLRP3 expressions and subsequent IL-1 $\beta$  and IL-18 release under LPS stimulation, while inhibition of autophagy by 3-MA enhanced NLRP3 expressions in macrophage. It has been reported that electro acupuncture could inhibit the activation of NLRP3 inflammasome through stimulating CB2, which suggest a signaling pathway between CB2 and NLRP3 (36). Our study also showed that inhibiting NLRP3 may be involved in the inhibitory effect of inflammatory responses by autophagy induction through CB2 activation.

In consistent with the results of *in vivo* CLP-induced ALI model, CB2 activation resulted in significant increasing autophagy, which could inhibit the release of TNF- $\alpha$ , IL-18 and IL-1 $\beta$  in our *in vitro* model. Furthermore, decreases in inflammatory response caused by CB2 activation were aggravated with 3-MA treatment.

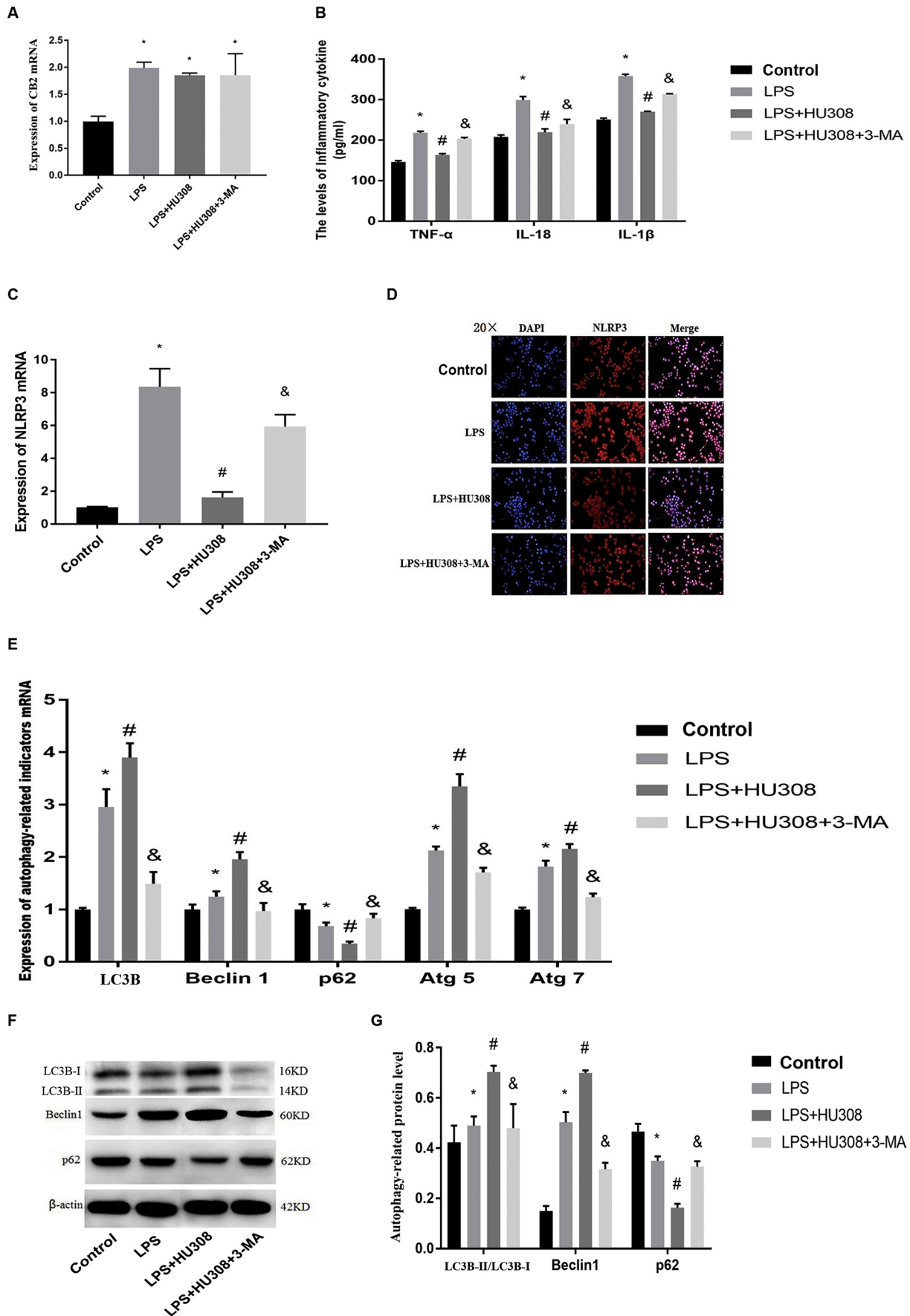
In summary, in this study we found that CB2 activation has a protective effect in a model of CLP-induced sepsis. CB2 activation increases the survival of mice and improves ALI induced by CLP through enhancement of autophagy. Moreover, the present study highlights autophagy as a major signaling pathway in the anti-inflammatory effect of CB2 in CLP-induced sepsis and LPS-stimulated macrophages. However, given the importance of inflammasome activation in sepsis, further mechanistic studies are warranted to investigate the molecular mechanism of autophagy in NLRP3 inflammasome activation.

#### Declaration of Competing Interest

The authors declare that they have no conflict of interest.

#### Acknowledgements

This work was supported by grants from National Natural Science Foundation of China (grant number 81101408), Hubei Provincial Natural Science Foundation of China (grant number 2019CFB690), Science and Technology Innovation Foundation of Zhongnan Hospital of Wuhan University (grant number znpzy2018109) and Fundamental



(caption on next page)

**Fig. 4.** The levels of inflammatory mediators in LPS-stimulated RAW264.7 macrophages were decreased by activating CB2, but this process is blocked by inhibition of autophagy.

RAW264.7 macrophages and cell supernatant were collected to measure inflammatory factors and autophagy-related indicators. (A) The expression of CB2 mRNA was up-regulated after LPS administration. (B) The level of TNF- $\alpha$ , IL-18 and IL-1 $\beta$  in cell supernatant was measured by ELISA. (C-D) The expression of NLRP3 was measured by qRT-PCR and immunofluorescence analysis. Magnification: 20 $\times$ , Scale bar: 20  $\mu$ m. (E-G) The expression of autophagy-associated indicator LC3B, Beclin1 and p62 was measured by qRT-PCR and Western blot analysis, as well as Atg5 and Atg7 were measured by qRT-PCR. Data are represented as mean  $\pm$  SD (n = 3–5), \*P < 0.05 versus control group; #P < 0.05 versus LPS group; &P < 0.05 versus CLP + HU308 group. CB2: Cannabinoid receptor 2; LPS: lipopolysaccharide.

Research Funds for the Central Universities of China (grant number 2042018kf0158).

## References

- [1] R. Al-Zoubi, P. Morales, P.H. Reggio, Structural insights into CB1 receptor biased signaling, *Int. J. Mol. Sci.* 20 (8) (2019) (pii: E1837).
- [2] R. Androvicova, J. Horacek, T. Stark, et al., Endocannabinoid system in sexual motivational processes: is it a novel therapeutic horizon? *Pharmacol. Res.* 115 (2017) 200–208.
- [3] J. Sardinha, M.E.M. Kelly, J. Zhou, et al., Experimental cannabinoid 2 receptor-mediated immune modulation in Sepsis, *Mediat. Inflamm.* 2014 (2014) 978678.
- [4] P. Pacher, S. Steffens, G. Haskó, et al., Cardiovascular effects of marijuana and synthetic cannabinoids: the good, the bad, and the ugly, *Nat. Rev. Cardiol.* 15 (3) (2018) 151–166.
- [5] S. Fechtner, A.K. Singh, I. Srivastava, et al., Cannabinoid receptor 2 agonist JWH-015 inhibits interleukin-1 $\beta$ -induced inflammation in rheumatoid arthritis synovial fibroblasts and in adjuvant induced arthritis rat via glucocorticoid receptor, *Front. Immunol.* 10 (2019) 1027.
- [6] C. Matyas, K. Erdelyi, E. Trojnar, et al., Interplay of liver-heart inflammatory axis and cannabinoid 2 receptorsignalling in an experimental model of hepatic cardiomyopathy, *Hepatology* (2019 Aug 30), <https://doi.org/10.1002/hep.30916>.
- [7] H. Gui, Y. Sun, Z.M. Luo, et al., Cannabinoid receptor 2 protects against acute experimental sepsis in mice, *Mediat. Inflamm.* 2013 (2013) 741303.
- [8] J. Tschöp, K.R. Kasten, R. Nogueiras, et al., The cannabinoid receptor 2 is critical for the host response to sepsis, *J. Immunol.* 183 (1) (2009) 499–505.
- [9] M. Trinder, J.H. Boyd, L.R. Brunham, Molecular regulation of plasma lipid levels during systemic inflammation and sepsis, *Curr. Opin. Lipidol.* 30 (2) (2019) 108–116.
- [10] I. Park, M. Kim, K. Choe, et al., Neutrophils disturb pulmonary microcirculation in sepsis-induced acute lung injury, *Eur. Respir. J.* 53 (3) (2019) (pii: 1800786).
- [11] X. Chen, Y. Wang, X. Xie, et al., Heme Oxygenase-1 reduces Sepsis-induced endoplasmic reticulum stress and ALI, *Mediat. Inflamm.* b2018 (2018) 9413876.
- [12] I. Cinar, B. Sirin, P. Aydin, et al., Ameliorative effect of gossypin against ALI in experimental sepsis model of rats, *Life Sci.* 221 (2019) 327–334.
- [13] N.M. Kocaturk, Y. Akkoc, C. Kig, et al., Autophagy as a molecular target for cancer treatment, *Eur. J. Pharm. Sci.* 134 (2019) 116–137.
- [14] P. Wang, T.M. Nolan, Y. Yin, et al., Identification of transcription factors that regulate ATG8 expression and autophagy in Arabidopsis, *Autophagy* 25 (2019) 1–17.
- [15] S.F. Nabavi, A. Sureda, A. Sanches-Silva, et al., Novel therapeutic strategies for stroke: the role of autophagy, *Crit. Rev. Clin. Lab. Sci.* 1 (2019) 1–18.
- [16] J. Ho, J. Yu, S.H. Wong, et al., Autophagy in sepsis: degradation into exhaustion? *Autophagy* 12 (7) (2016) 1073–1082.
- [17] H. Zhao, H. Chen, M. Xiaoyin, et al., Autophagy activation improves lung injury and inflammation in Sepsis, *Inflammation* 42 (2) (2019) 426–439.
- [18] J.Y. Chen, S. Min, F. Xie, et al., Enhancing autophagy protects against Sepsis-induced neuromuscular dysfunction associated with qualitative changes to acetylcholine receptors, *Shock* 52 (1) (2019) 111–121.
- [19] T. Denaës, J. Lodder, M.N. Chobert, et al., The cannabinoid receptor 2 protects against alcoholic liver disease via a macrophage autophagy-dependent pathway, *Sci. Rep.* 6 (2016) 28806.
- [20] D. Rittirsch, M.S. Huber-Lang, M.A. Flierl, et al., Immunodesign of experimental sepsis by cecal ligation and puncture, *Nat. Protoc.* 4 (1) (2009) 31–36.
- [21] K.M. Smith, J.D. Mrozek, S.C. Simonton, Prolonged partial liquid ventilation using conventional and high-frequency ventilatory techniques: gas exchange and lung pathology in an animal model of respiratory distress syndrome, *Crit. Care Med.* 25 (11) (1997) 1888–1897.
- [22] J.D. Pressly, H. Soni, S. Jiang, et al., Activation of the cannabinoid receptor 2 increases renal perfusion, *Physiol. Genomics* 51 (3) (2019) 90–96.
- [23] Q. He, F. Xiao, Q. Yuan, et al., Cannabinoid receptor 2: a potential novel therapeutic target for sepsis? *Acta Clin. Belg.* 74 (2) (2019) 70–74.
- [24] A. Meza, C. Lehmann, Betacaryophyllene –a phytocannabinoid as potential therapeutic modality for human sepsis? *Med. Hypotheses* 110 (2018) 68–70.
- [25] K. Wilhelmens, S. Khakpour, A. Tran, et al., The endocannabinoid/endovanilloid N-arachidonoyl dopamine (NADA) and synthetic cannabinoid WIN55, 212-2 abate the inflammatoryactivation of human endothelial cells, *J. Biol. Chem.* 289 (19) (2014) 13079–13100.
- [26] F. Montecucco, F. Burger, F. Mach, et al., CB2 cannabinoid receptor agonist JWH-015 modulates human monocyte migration through defined intracellular signaling pathways, *Am. J. Physiol. Heart Circ. Physiol.* 294 (3) (2008) H1145–H1155.
- [27] F. Molica, C.M. Matter, F. Burger, et al., Cannabinoid receptor CB2 protects against balloon-induced neointima formation, *Am. J. Physiol. Heart Circ. Physiol.* 302 (5) (2012) H1064–H1074.
- [28] A.M. Malfitano, C. Laezza, S. Bertini, et al., Immunomodulatory properties of 1, 2-dihydro-4-hydroxy-2-oxo-1,8-naphthyridine-3-carboxamide derivative VL15, *Biochimie* 135 (2017) 173–180.
- [29] C. Lehmann, M. Kianian, J. Zhou, et al., Cannabinoid receptor 2 activation reduces intestinal leukocyte recruitment and systemic inflammatory mediator release in acute experimental sepsis, *Crit. Care* 16 (2) (2012) R47.
- [30] L. Rao, N.T. Eissa, Autophagy in pulmonary innate immunity, *J. Innate Immun.* 24 (2019) 1–10.
- [31] N. Tilija Pun, P.H. Park, Adiponectin inhibits inflammatory cytokines production by Beclin-1 phosphorylation and B-cell lymphoma 2 mRNA destabilization: role for autophagy induction, *Br. J. Pharmacol.* 175 (7) (2018) 1066–1084.
- [32] Y. Zhang, L. Wang, L. Meng, et al., Sirtuin 6 overexpression relieves sepsis-induced acute kidney injury by promoting autophagy, *Cell Cycle* 18 (4) (2019) 425–436.
- [33] C. Hiebel, C. Behl, The complex modulation of lysosomal degradation pathways by cannabinoid receptors 1 and 2, *Life Sci.* 138 (2015) 3–7.
- [34] Y. Hu, Y. Tao, J. Hu, Cannabinoid receptor 2 deletion deteriorates myocardial infarction through the down-regulation of AMPK-mTOR-p70S6K signaling-mediated autophagy, *Biosci. Rep.* 39 (4) (2019).
- [35] A. Wu, P. Hu, J. Lin, et al., Activating cannabinoid receptor 2 protects against diabetic cardiomyopathy through autophagy induction, *Front. Pharmacol.* 9 (2018) 1292.
- [36] P. Ke, B.Z. Shao, Z.Q. Xu, et al., Activation of cannabinoid receptor 2 ameliorates DSS-induced colitis through inhibiting NLRP3 Inflammasome in macrophages, *PLoS One* 11 (9) (2016) e0155076.
- [37] J. Chen, S. Wang, R. Fu, et al., RIP3 dependent NLRP3 inflammasome activation is implicated in ALI in mice, *J. Transl. Med.* 16 (1) (2018) 233.
- [38] M. Saleh, The machinery of nod-like receptors: refining the paths to immunity and cell death, *Immunol. Rev.* 243 (2011) 235–246.
- [39] F. Gao, H.C. Xiang, H.P. Li, et al., Electroacupuncture inhibits NLRP3 inflammasome activation through CB2 receptors in inflammatory pain, *Brain Behav. Immun.* 67 (2018) 91–100.